INTERNATIONAL JOURNAL FOR NUMERICAL METHODS IN FLUIDS, VOL. 4, 667–683 (1984)

DEVELOPMENT OF A COMPUTER PROGRAM FOR THE PREDICTION OF FLOW IN A ROTATING CAVITY

J. W. CHEW

Theoretical Science Group, Rolls-Royce Limited, Derby, England

SUMMARY

A computer program has been developed to predict laminar source–sink flow in a rotating cylindrical cavity. Although the program is based on a standard finite difference technique for recirculating flow, it incorporates two novel features. Step changes in grid size are employed to obtain sufficient resolution in the boundary layers and special treatment is given to the solution of the pressure correction equations, in the 'SIMPLE' algorithm, in order to improve the convergence properties of the method. Results are presented both for the flow in an infinite rotating cylindrical annulus and a finite rotating cylindrical cavity, with the inner cylindrical surface acting as a uniform source and the outer cylinder as a sink. These show good agreement with existing analytical solutions and illustrate some of the problems associated with the computation of rapidly rotating flows.

KEY WORDS Rotating Flow Finite Differences Numerical Stability

1. INTRODUCTION

A problem of interest in gas turbine design is the flow of cooling air between co-rotating discs, and in recent years this has been the subject of considerable experimental research (see, for example, Reference 1). This paper records the development of a computer program for the prediction of such flows. Emphasis is placed on the behaviour of the numerical scheme, rather than the flow structure, which will be discussed in a subsequent paper.

One of the first numerical studies of flow in a rotating cavity was by Pao,[2] who considered the flow caused by one of the discs being held stationary, while the other surface rotated. The highest value of the rotational Reynolds number ($Re_\theta = \Omega b^2/\nu$) for which he was able to obtain results was 200. Above this, the slow rate of convergence of the iterative solution of the finite difference equations made the computation impracticable. Similar difficulties to this have since been experienced by several other workers who have used a variety of different methods to solve the finite difference equations for laminar flow. For the flow in a cavity formed by two rotating discs and a fixed cylindrical shroud, Gosman and Spalding[3] obtained results for $Re_\theta = 10^3$. Bennetts and Jackson[4] obtained solutions for source–sink flow in a rotating cavity with $Re_\theta = 3{\cdot}5 \times 10^3$, and Harada[5] has produced results for thermally driven flow in rotating cavity with $Re_\theta = 10^3$.

Finite element methods have recently been applied to a variety of different laminar flows by Bar-Yoseph, Blech and Solan.[6] The main advantage of this method over finite difference techniques appears to be its versatility in accounting for different boundary shapes. The problem of convergence of the solution at high rotational speeds remains.

0271-2091/84/070667-17$01.70

Received 29 September 1982
Revised 20 June 1983

Since none of the methods used by the workers mentioned above appears to have a distinct advantage over the others for the computation of rapidly rotating flow it was decided, in the present study, to adapt the readily available 'TEACH' program, developed by Gosman and Ideriah,[7] for rotating flow. The finite difference methods used in this program have been tested on a wide range of non-rotating flows and were used by Gosman *et al.*[8] to study turbulent flow between a rotating and a stationary disc.

In Sections 2 and 3 the standard numerical methods and the modifications that have been made to these methods are described. Application of the computer program is then illustrated in Sections 4 and 5 and the results are discussed in Section 6. The notation used is given in the Appendix.

2. THE FINITE DIFFERENCE FORMULATION

2.1. *The governing equations*

For laminar flow, with the assumption of axisymmetry and constant viscosity, the three momentum equations and the continuity equation can be written:

$$\frac{1}{r}\frac{\partial(\rho r u^2)}{\partial r}+\frac{\partial(\rho u w)}{\partial z}=-\frac{\partial p'}{\partial r}+\mu\left[\frac{1}{r}\frac{\partial}{\partial r}\left(r\frac{\partial u}{\partial r}\right)+\frac{\partial^2 u}{\partial z^2}-\frac{u}{r^2}\right]+2\rho\Omega v+\frac{\rho v^2}{r} \tag{1}$$

$$\frac{1}{r}\frac{\partial(\rho r u v)}{\partial r}+\frac{\partial(\rho v w)}{\partial z}=\mu\left[\frac{1}{r}\frac{\partial}{\partial r}\left(r\frac{\partial v}{\partial r}\right)+\frac{\partial^2 v}{\partial z^2}-\frac{v}{r^2}\right]-\frac{\rho u v}{r}-2\rho\Omega u \tag{2}$$

$$\frac{1}{r}\frac{\partial(\rho r u w)}{\partial r}+\frac{\partial(\rho w^2)}{\partial z}=-\frac{\partial p'}{\partial z}+\mu\left[\frac{1}{r}\frac{\partial}{\partial r}\left(r\frac{\partial w}{\partial r}\right)+\frac{\partial^2 w}{\partial z^2}\right] \tag{3}$$

$$\frac{1}{r}\frac{\partial(r u)}{\partial r}+\frac{\partial w}{\partial z}=0 \tag{4}$$

where p' is the reduced pressure defined by

$$p'=p-\tfrac{1}{2}\rho\Omega^2 r^2 \tag{5}$$

Here (u, v, w) is the velocity relative to a cylindrical co-ordinate system (r, ϕ, z) rotating at angular velocity Ω.

The three momentum equations, (1)–(3) can be expressed in terms of a common equation:

$$\frac{1}{r}\frac{\partial}{\partial r}(r\rho u\Phi)+\frac{\partial}{\partial z}(\rho w\Phi)=\frac{1}{r}\frac{\partial}{\partial r}\left(\mu r\frac{\partial\Phi}{\partial r}\right)+\frac{\partial}{\partial z}\left(\mu\frac{\partial\Phi}{\partial z}\right)+S_\Phi \tag{6}$$

where Φ represents one of the three velocity components, u, v or w, and the source term, S_Φ, is different for each variable.

2.2. *Finite difference representation on a uniform grid*

Derivation of the finite difference equations for a uniform grid follows the standard method described by Patankar and Spalding.[9] A staggered finite difference grid is used, as shown in Figure 1. The radial and axial velocities are calculated at the points marked ↑ and →, respectively, on this diagram. Other variables are calculated at the main grid points. A control volume is associated with each grid point and the finite difference equations are obtained by integration over the control volumes.

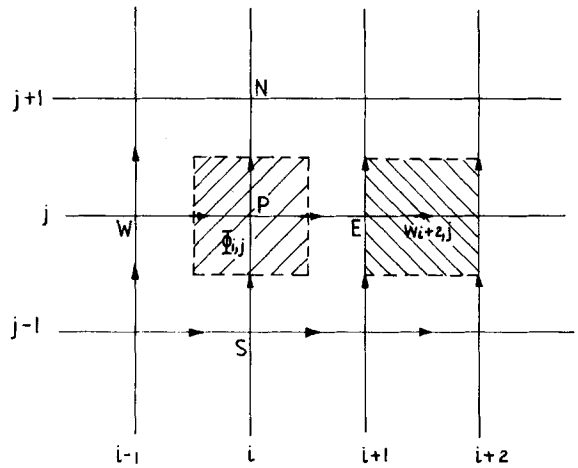

Figure 1. Control volumes for $\Phi_{i,j}$ /// and $w_{i+2,j}$ \\\

The finite difference representation of equation (6) at the point P has the form

$$c_P\Phi_P = \sum_K c_K\Phi_K + (S_1 + S_2\Phi_P) \tag{7}$$

where $\sum_K$ represents the summation over the four neighbouring points, N, S, E and W, and Φ can represent any of the velocity components u, v or w. The coefficients in (7) are of standard form and details can be found elsewhere.[10] Hybrid differencing is used for the convective terms.

The continuity equation requires special treatment, as it is used in the iterative solution method to obtain improved values of the pressure. It is sufficient to note here that pressure correction equations of the form (7) can be derived and solution of these equations ensures that mass balances for the control volumes associated with the main grid points are satisfied.

2.3. *Finite difference representation for a step change in grid spacing*

Provided that constant mesh spacings δr and δz are used, the truncation error of the above scheme is second order when central differencing is employed, and first order when upwind differencing is used. Extension of this method to a non-uniform grid is straightforward but care must be taken to ensure that 'correct' values of the variables at the control volume boundaries are used, and the truncation error will be first order. Roache[11] has discussed the problem of introducing a change in mesh size and has shown that unless the spacing is changed slowly the formal truncation error of the standard method may actually be deteriorated rather than improved. As, for the flows studied here, some kind of variable grid was essential, it was decided, considering Roache's observations, to incorporate a step change in mesh size in the solution procedure. This avoids some of the complications of a gradually variable grid and allows special treatment of the point at which the mesh size increases, so that the truncation error will not be inadvertently increased.

If the factor by which the mesh size is increased or decreased is restricted to be an odd integer, a particularly simple method can be used to ensure that the order of the truncation error is not reduced at the point where the grid changes. This may be illustrated by considering an increase in mesh size in the z direction by a factor of three, as shown in

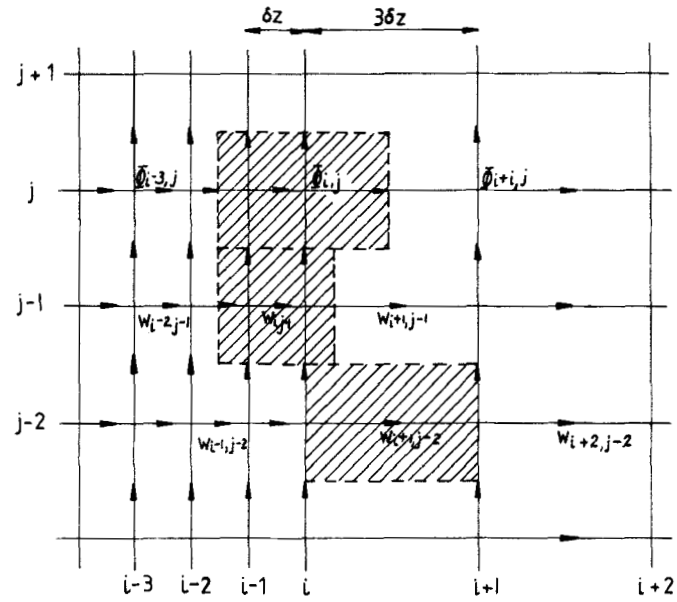

Figure 2. Grid change by factor 3 in the axial direction. The control volumes associated with $\Phi_{i,j}$, $w_{i,j-1}$ and $w_{i+1,j-2}$ are shown

Figure 2. This diagram shows the control volumes that are used to obtain the finite difference equations both for a variable on the main grid line and for the axial velocities either side of this line. Effectively, the equation for a variable ($\Phi_{i,j}$ say) on the main grid line is calculated as though the two points $\Phi_{i-1,j}$ and $\Phi_{i-2,j}$ (using the notation shown in the diagram), did not exist. As a result, the finite difference equation for $\Phi_{i,j}$ has the form

$$c_P\Phi_{i,j} = c_N\Phi_{i,j+1} + c_S\Phi_{i,j-1} + c_E\Phi_{i+1,j} + c_W\Phi_{i-3,j} + (S_1 + S_2\Phi_{i,j}) \tag{8}$$

This differs from the standard form by the inclusion of $\Phi_{i-3,j}$ instead of $\Phi_{i-1,j}$. The truncation error at this point is of the same order as if a constant mesh of size $3\delta z$ were used. Equations for the axial velocities $w_{i,j}$ and $w_{i-1,j}$ can be derived in a similar manner, again without deterioration in the truncation error. The equation for $w_{i,j}$ will have the form

$$c_P w_{i,j} = c_N w_{i,j+1} + c_S w_{i,j-1} + c_E w_{i+1,j} + c_W w_{i-2,j} + (S_1 + S_2 w_{i,j}) \tag{9}$$

and the equation for $w_{i+1,j}$ has the form

$$c'_P w_{i+1,j} = c'_N w_{i+1,j+1} + c'_S w_{i+1,j-1} + c'_E w_{i+2,j} + c'_W w_{i-1,j} + S'_1 + S'_2 w_{i+1,j} \tag{10}$$

where the superscript $'$ has been introduced to show that the coefficients in (9) and (10) are not equal.

This scheme has the advantages that the formal truncation error is not increased and it fits in well with the control volume approach. However it should be noted that it does restrict the change in grid size to a factor of an odd integer and requires some modification of the standard solution procedure.

3. SOLUTION OF THE FINITE DIFFERENCE EQUATIONS

3.1. *The standard 'SIMPLE' method*

In this well known algorithm the estimates for u, v, w and p are successively updated by solution of equations of the form (7). A 'line-by-line' (l.b.l.) procedure, which is an ADI type method employing alternate 'sweeps' in the axial and radial directions, is used for each solution of this equation.

To ensure that the iterative procedure converges to the solution of the difference equations, under-relaxation factors are introduced for each of the four variables. Gosman *et al.*[8] also used another form of relaxation. They suggested that the term

$$\alpha \frac{\rho}{r}(\Omega r + v)(u_{\text{old}} - u_{\text{new}}) \tag{11}$$

where α is a constant, should be added to the right-hand-side of the radial momentum equation. The motivation for this is that there are strong links between the radial and azimuthal momentum equations and if u increases, a decrease in v is expected and so the centrifugal force term in the radial equation should be reduced.

The standard criterion, used to determine whether or not the solution had converged is based on residuals for each of the four conservation equations. These are calculated from the relation

$$R = \sum |(c_P - S_2)\Phi_P - c_N\Phi_N - c_S\Phi_S - c_E\Phi_E - c_W\Phi_W - S_1| \tag{12}$$

where the summation is carried out over all points P of the finite difference grid. As the residuals should be equal to zero for the exact solution the computation is stopped if the residuals all fall below some prescribed value. In the present work it was found that a suitable cut-off point which gave reasonable convergence for all cases did not lead to excessive computing time was difficult to define. In effect the residuals were used as a guide to show whether or not the solution was improving and computations were stopped when further reduction in the residuals appeared to produce only small changes (relative to some typical value) in the velocities and pressure.

3.2. *Treatment of the equations at a step change in the grid*

As the finite difference equations for the nodes at which a change in mesh spacing occurs do not fit into the standard form, the l.b.l. solution procedure cannot be applied directly at these points. To illustrate how these non-standard equations are incorporated into the solution method, consider equation (8), together with the equations for $\Phi_{i-1,j}$ and $\Phi_{i-2,j}$. In the l.b.l. solution method mentioned earlier, when a sweep is made in the radial direction, the values of Φ along the axial lines $j-1$ and $j+1$ are assumed known so that at this stage the equations can be written

$$\begin{aligned} A\Phi_{i,j} &= B\Phi_{i+1,j} + C\Phi_{i-3,j} + D \\ A'\Phi_{i-1,j} &= B'\Phi_{i,j} + C'\Phi_{i-2,j} + D' \\ A''\Phi_{i-2,j} &= B''\Phi_{i-1,j} + C''\Phi_{i-3,j} + D'' \end{aligned} \tag{13}$$

The second of these equations can be used to eliminate $\Phi_{i-2,j}$ from the third which is then used to eliminate $\Phi_{i-3,j}$ from the first. The resulting equation is

$$\left(A+\frac{CA''B'}{C''C'}\right)\Phi_{i,j}=B\Phi_{i+1,j}+\frac{C}{C''}\left(\frac{A''A'}{C'}-B''\right)\Phi_{i-1,j}+D-\frac{C}{C''}\left(D''+\frac{D'A''}{C'}\right) \tag{14}$$

If this equation is used in place of the original equation for $\Phi_{i,j}$ the tridiagonal matrix algorithm can be used as before. A similar procedure is used for the sweep in the opposite direction when there is a change in the radial mesh size.

3.3. Special treatment of the pressure correction equations

Owing to the non-linearity and coupling of the governing equations the iterative scheme described above does not always converge. The solution may oscillate or diverge, resulting in an overflow error on the computer. As mentioned previously, under-relaxation may be used to try to obtain convergence. Gosman *et al.*[8] report that the provision of good initial estimates and the gradual introduction of high swirl rates also helps to avoid these instabilities. Unfortunately no general rule is known for estimating the optimal under-relaxation factors or the constant α in equation (11) and, as will be shown in Section 4, the method can be very sensitive to this choice. In the present work it was found that instabilities could be avoided, and the rate of convergence improved, by ensuring that the pressure correction terms, through which the velocities are corrected to ensure that the mass conservation equations are satisfied, were calculated to sufficient accuracy. Examples showing this effect are given in Section 5. The modifications to the l.b.l. procedure used to solve the pressure correction equations are described below.

Initially the accuracy of the pressure correction solution was improved simply by making more sweeps in the application of the l.b.l. procedure. As this proved expensive in the use of computer processing time, the method was modified so that, if the maximum variation in the pressure corrections between successive sweeps fell below a prescribed fraction of a representative pressure difference for the cavity, the l.b.l. method was stopped at that point. Subsequently it was found that use of an acceleration procedure could further improve convergence rates. A more suitable criterion to stop the iterations was then defined so that a mass residual, R_k, was reduced to a prescribed fraction of its starting value. This residual was calculated from the relation:

$$R_k=\sum|(c_P-S_2)pp_{P,k}-c_Npp_{N,k}-c_Spp_{S,k}-c_Epp_{E,k}-c_Wpp_{W,k}-S_1| \tag{15}$$

where the summation is carried out over all points P of the finite difference grid and the subscript k refers to values after k sweeps in each direction.

The acceleration method used is due to Aitken and is described by Smith.[12] An outline of the theoretical basis for the method is given here for completeness. To help understanding, it is useful to introduce matrix notation. The l.b.l. solution procedure may then be represented by the relation:

$$\mathbf{pp}_k=\mathbf{A}\mathbf{pp}_{k-1}+\mathbf{B}, \qquad k=1,2\ldots \tag{16}$$

where $\mathbf{A}$ and $\mathbf{B}$ are constant matrices and $\mathbf{pp}_k$ denotes the estimate of the pressure correction vector after k sweeps in each direction. It follows that:

$$\mathbf{e}_k=\mathbf{A}\mathbf{e}_{k-1}=\mathbf{A}^2\mathbf{e}_{k-2}=\ldots\mathbf{A}^k\mathbf{e}_0 \tag{17}$$

where

$$\mathbf{e}_k = \mathbf{pp}_{\text{true}} - \mathbf{pp}_k \tag{18}$$

and $\mathbf{pp}_{\text{true}}$ is the true solution for the pressure correction. Assuming that $\mathbf{A}$ is of order m and has m linearly independent eigenvectors $\mathbf{V}_1, \mathbf{V}_2, \ldots, \mathbf{V}_m$ it is possible to find constants $c_1, c_2, \ldots, c_m$ such that

$$\mathbf{e}_0 = \sum_{i=1}^{m} c_i \mathbf{V}_i \tag{19}$$

Substituting this expression into (17) and using the fact that $\mathbf{AV}_i = \lambda_i \mathbf{V}_i$ where λ_i is the eigenvalue corresponding to $\mathbf{V}_i$ gives

$$\mathbf{e}_k = \sum_{i=1}^{m} c_i \lambda_i^k V_i \tag{20}$$

Thus, for $k \gg 1$

where

$$\mathbf{e}_{k+1} \simeq \lambda_s \mathbf{e}_k \simeq \lambda_s^2 \mathbf{e}_{k-1} \tag{21}$$

$$|\lambda_s| = \max(|\lambda_1|, |\lambda_2|, \ldots, |\lambda_m|)$$

Substituting (18) into equation (21) and eliminating λ_s gives, after some manipulation,

$$pp_{\text{true}} = pp_{k+1} - \frac{(pp_{k+1} - pp_k)^2}{pp_{k+1} - 2pp_k + pp_{k-1}} \tag{22}$$

for any component pp_{true} of $\mathbf{pp}_{\text{true}}$. In practice, equation (22) is used after a certain number of iterations to provide improved values for subsequent iterations.

Figure 3 shows how the solution of the pressure correction equations can be improved by using the acceleration procedure. This particular example was taken from a program run for flow in a cylindrical cavity, including end effects, with a radial source and sink at a Reynolds number (Re_θ) of 5×10^4 and the mass flow parameter (C_w) equal to 192. The modulus of the maximum eigenvalue of the iteration matrix, as estimated from the slope of the curve for the standard algorithm in this figure, is approximately 0·99. As can be seen from equation (21) this indicates that the change in the values of the pressure corrections during each iteration may be small while the error in the solution is still significant. Although it is clear that use of the acceleration procedure considerably improves the rate of convergence, the optimum point at which the procedure should be applied will depend on the criterion used to stop the iterations.

4. ONE-DIMENSIONAL SOURCE–SINK FLOW

An exact analytical solution for flow in an infinite rotating cylindrical annulus with the inner cylindrical surface acting as a uniform source and the outer cylinder as a uniform sink has been derived by Hide.[13] So that numerical results could be compared with this solution the boundary conditions in the computer program are taken as

$$\begin{aligned} &u = \frac{Q}{2\pi r s}, \qquad v = w = 0 \quad \text{at} \quad r = a, b \\ &\frac{\partial u}{\partial z} = \frac{\partial v}{\partial z} = \frac{\partial w}{\partial z} = \frac{\partial p}{\partial z} = 0 \quad \text{at} \quad z = 0, s \end{aligned} \tag{23}$$

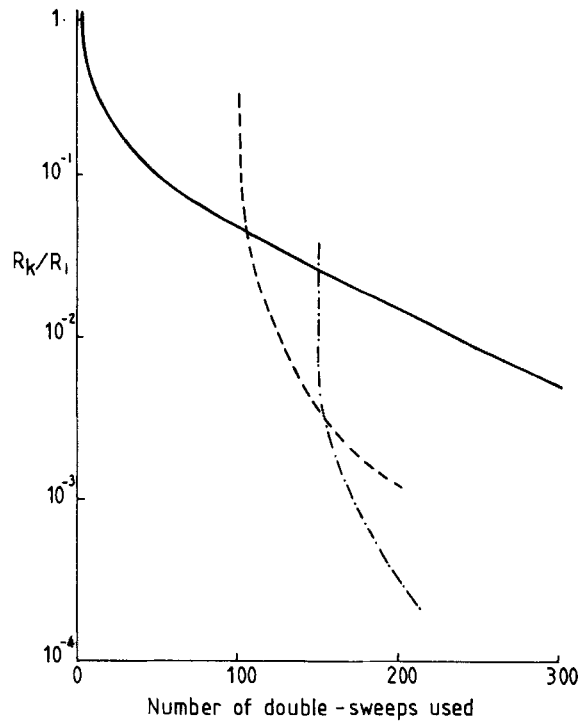

Figure 3. Use of Aitken's acceleration method in the line-by-line solution algorithm: ——— standard algorithm; - - - - - - acceleration procedure applied after 100 double-sweeps; - · - · - acceleration procedure applied after 150 double-sweeps

Program runs were then made for several different rotational speeds and mass flow rates with the highest rotational and source Reynolds numbers ($Re_\theta = \Omega b^2/\nu$, $S = Q/2\pi\nu s$) being 8170 and 34, respectively. Good agreement between numerical and analytical solutions was obtained. An example of the results is given in Figure 4 which shows a comparison of the analytical and numerical predictions for the tangential velocity when $Re_\theta = 4085$, $S = 34$. The finite difference grid used in these computations gave the results at four equally spaced axial positions while, as can be seen from the graph, several different radial grid spacings were used. These results show how a change in mesh size can be employed to give a better description of the flow in the boundary layer on the sink.

It was apparent from the computations that, as the rotational speed was increased, so convergence of the iterative solution method became more difficult to obtain and more computing time was required. To investigate how this problem might be alleviated it was decided to test the sensitivity of the method to various parameters. Since it was desirable to minimize the computing time used, the analytically trivial case $S = 0$ was chosen for this investigation. In this case the solution reduces to 'solid body rotation' ($u = v = w = 0$) and so only a small number of grid points are needed for the numerical solution to give the exact result. For the examples described below a 4×4 grid was used and the starting values for the calculations were for the fluid at rest ($u = w = 0$, $v = -\Omega r$).

Figure 5 shows the effect of varying the under-relaxation factors for the tangential velocity and pressure for the case $Re_\theta = 5515$, $S = 0$, with all other parameters held constant. These graphs give the variation of the tangential velocity at an interior point during the course of

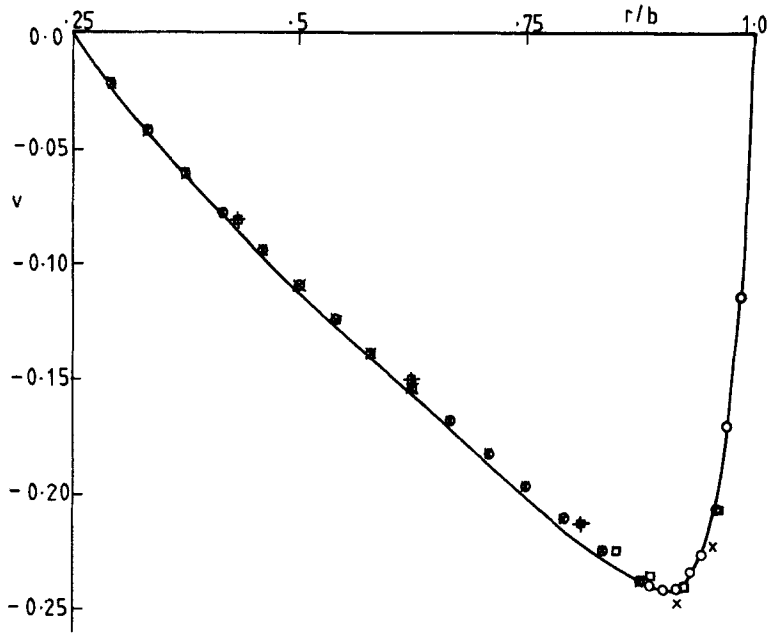

Figure 4. One-dimensional source–sink flow. $Re_\theta = 4085$, $S = 34$. Tangential velocity vs. radial position. Exact analytical solution (———). Numerical results: (a) + uniform grid, 3 interior points; (b) □ non-uniform grid, δr decreased by factor 5 near the sink wall, 7 interior points; (c) × uniform grid, 17 interior points; (d) ○ non-uniform grid, δr decreased by factor 3 near the sink wall, 23 interior points

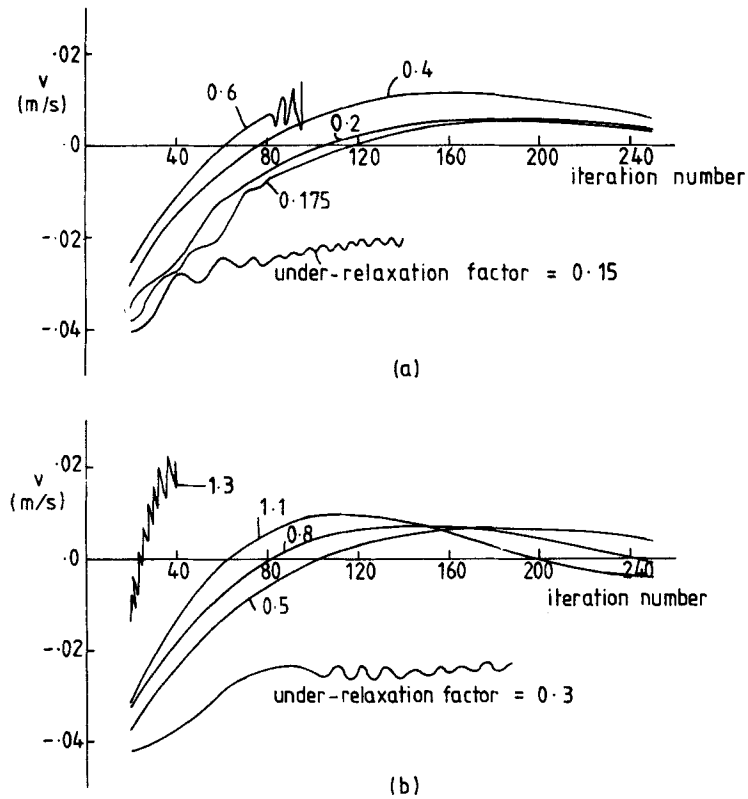

Figure 5. Effect of under-relaxation factors on the computation of the tangential velocity, at one reference point, during solid-body rotation ($Re_\theta = 5515$): (a) the effect of the under-relaxation of v; (b) the effect of the under-relaxation of p

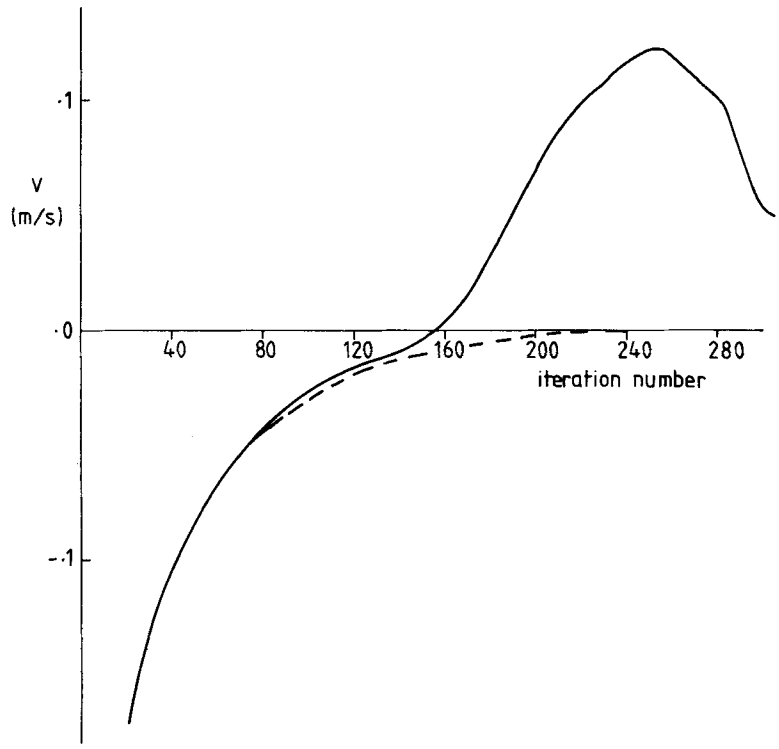

Figure 6. Effect of the number of sweeps on the computation of the tangential velocity, at one reference point, during solid-body rotation ($Re_\theta = 27{,}500$): —— one sweep in each direction; ---- three sweeps in each direction

the calculations. Typically the value would oscillate slowly about the exact solution with the amplitude of the oscillations decreasing as the calculation proceeded. Note that an 'under-relaxation' factor greater than unity corresponds to the use of over-relaxation. The results indicate that problems can arise if the factors are either too high or too low. When too high a value was used, the solution oscillated wildly and eventually gave rise to arithmetic overflow. When too low a value was used, the solution oscillated slowly and appeared to creep towards the exact solution. The computation was not carried on long enough to determine whether the exact solution would ever be reached. The effect of the factors for axial and radial velocities and the parameter α in equation (11) was not considered, as the starting values for u and w already satisfied the required solution.

In the earlier computations it was noticed that a particularly effective method of procuring convergence was to increase the number of sweeps used in the l.b.l. solution method described above. To isolate this effect two program runs were made for $Re_\theta = 27{,}500$, $S = 0$, in which the only difference was a variation in this parameter. Figure 6 shows the behaviour of tangential velocity at the interior reference point during each run. When just one sweep in each direction was employed, the solution had not converged after 400 iterations, but when three double-sweeps were allowed an accurate result was achieved in 250 iterations. Note also that for the first 140 iterations there is very little difference between the two runs. It is only after this stage that the extra sweeps are needed to obtain convergence.

5. TWO-DIMENSIONAL SOURCE–SINK FLOW

In this section numerical results are given for the case of radial outflow of air through a rotating cylindrical cavity where the fluid enters the cavity from a central uniform cylindrical source and leaves through a uniform sink at the outer radius. Since the flow is symmetric about the mid-axial position, the solution domain was restricted to $0 \leq z \leq s/2$, and the boundary conditions were set to

$$\begin{aligned} u &= \frac{Q}{2\pi rs}, \qquad v = w = 0 \quad \text{at} \quad r = a, b \\ u &= v = w = 0 \quad \text{at} \quad z = 0 \\ \frac{\partial u}{\partial z} &= \frac{\partial v}{\partial z} = w = \frac{\partial p}{\partial z} = 0 \quad \text{at} \quad z = s/2 \end{aligned} \tag{24}$$

The following geometrical parameters were used: $a = 19$ mm, $b = 190$ mm, $\delta = 50{\cdot}7$ mm. The density and viscosity of air were taken as $\rho = 1{\cdot}225$ kg/m^3, $\mu = 1{\cdot}78 \times 10^{-5}$ kg/ms.

To confirm the validity of the numerical results the first case studied was for conditions in which Hide's[13] analytical solution for this class of flow is expected to be almost exact. The rotational Reynolds number was taken as $2{\cdot}5 \times 10^4$ and the mass flow parameter C_w was set at 0·01. Several program runs were made for these conditions using different finite difference grids. Some of the results are shown in Figure 7. The effect of grid size is shown in Figure

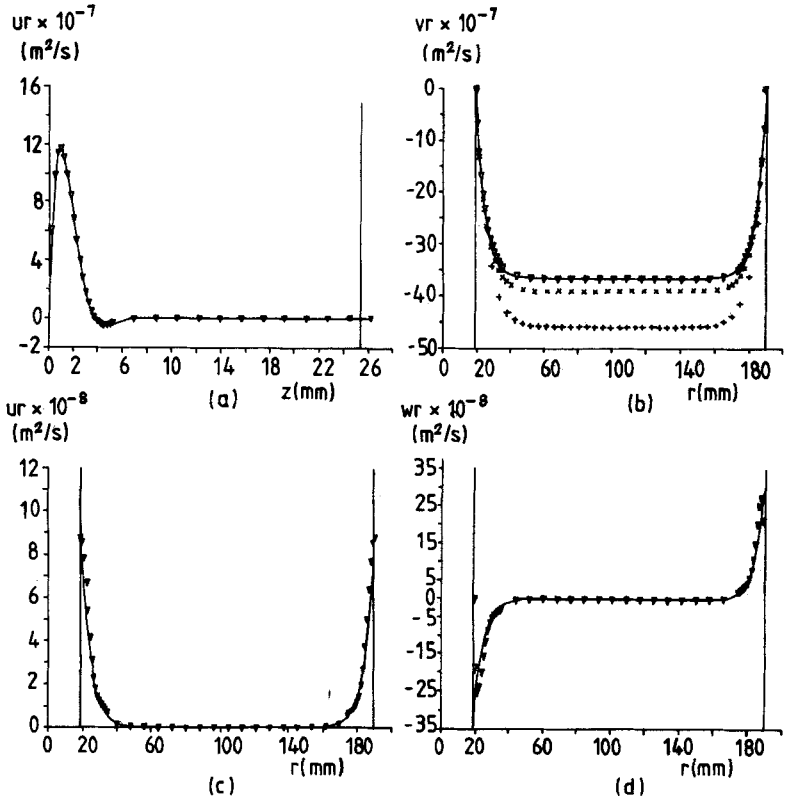

Figure 7. Two-dimensional source–sink flow. $Re_\theta = 2{\cdot}5 \times 10^4$, $C_w = 0{\cdot}01$, $b/a = 10$. Numerical results: ▽ non-uniform 34×46 grid; × non-uniform 22×37 grid; + uniform 22×37 grid. Hide (Reference 13) ———. (a) Axial variation of ur at $r = 105$ mm; (b) radial variation of vr on mid-axial plane; (c) radial variation of ur on mid-axial plane; (d) radial variation of wr at $z = 4{\cdot}1$ mm

7(b), which gives a comparison of the analytical solution for the tangential velocity and the computer predictions for three different grids. These results show how changes in grid size at each of the three boundary layers can be used to reduce the truncation error without a prohibitive increase in the total number of grid points. With a uniform grid having 22 points, in the axial direction and 37 points in the radial direction, the truncation error was quite large, as can be seen from the graphs. However, when the same number of grid points were distributed non-uniformly with the finer mesh size in the boundary layers, the error was considerably reduced. To confirm that the numerical solution did converge to the analytical solution, a run was made using a non-uniform grid with 34 points in the axial direction, and 46 in the radial direction. As can be seen from the velocity profiles for this case, excellent agreement was obtained. The slightly thicker boundary layer on the source given by the numerical results in Figures 7(b) and 7(c) could well be due to curvature effects which were neglected in Hide's solution. As the analytical approach also neglects the no slip condition on the axial velocity at $r = a$ and b some difference is to be expected close to these walls.

As for the one-dimensional flows described above, increasing the number of sweeps in the l.b.l. algorithm tended to improve the convergence rate for the solution. Further tests showed that this improvement was brought about by the more accurate solution of the pressure correction terms and that there was no benefit in increasing the number of sweeps made for the other variables. Thus the program was modified to allow only one double-sweep in the calculations for u, v and w but, as described in Section 3.3, give special treatment to the pressure corrections.

The effect of using different criteria for terminating the l.b.l. solution for the pressure terms was investigated for the case $Re_\theta = 5 \times 10^4$, $C_w = 192$, and some results from this study are shown in Table I. The starting values for these program runs correspond to solid body rotation at twice the rotational speed of the disc, the under-relaxation factors for the four variables were set at 0·5 and the constant α was set to zero. A non-uniform grid was used with 32 and 46 points in axial and radial directions. The degree of convergence obtained after 50 iterations in each case can be judged from the relative values of residuals for the three momentum equations and the continuity equation. For case 1, in which 100 double-sweeps were used for each calculation of the pressure corrections, the values of the residuals were found to have increased from the initial values and so it is unlikely that convergence will be obtained. The results for cases 2 and 3 show that convergence may be obtained by simply increasing the number of sweeps allowed. In case 4, the maximum number of double-sweeps used was 200, but the l.b.l. procedure was also stopped if the maximum change in the pressure correction terms during the last iteration was less than 0·05 per cent of the radial pressure difference across the cavity. Comparison of the results with case 2 shows that use of this criterion gives a considerable reduction in the computing time used, while the effect on convergence is small. For cases 5 and 6, the l.b.l. procedure was stopped when the mass residual was reduced to 5 per cent of its initial value or when 500 double-sweeps had been made. In case 6, Aitken's acceleration method was used after every hundred double-sweeps. The results indicate that the reduction of the residual to a certain percentage of its initial value is a reasonable criterion to use in the solution of the pressure correction equations. It would appear that Aitken's acceleration method not only gives a considerable saving in computing time but also results in better overall convergence. After further numerical experiments for various types of flow it was found that a single application of the acceleration method after a set number of double-sweeps (typically 200), with the termination of the procedure when either the residual was reduced to 5 per cent of its initial value or the number of sweeps reached a maximum value (typically 250), was the most useful

Table I. Effect of different methods of applying the line-by-line (l.b.l.) method to the solution of the pressure correction terms

Case No.	Criteria for stopping l.b.l. solution of pressure corrections	Normalized residuals after 50 iterations				*CPU time (s) for 50 iterations
		Axial momentum	Radial momentum	Tangential momentum	Mass	
1	100 double-sweeps allowed	$1{\cdot}67\times10^{4}$	$1{\cdot}06\times10^{4}$	1·85	276	204
2	200 double-sweeps allowed	2·69	2·50	2·21	0·56	397
3	300 double-sweeps allowed	1·69	1·72	2·70	1·24	594
4	(a) 200 double-sweeps allowed (b) iterations stopped if maximum change in pressure correction during an iteration <0·05 per cent of the pressure difference across cavity	2·85	2·60	2·25	0·56	204
5	(a) 500 double-sweeps allowed (b) iterations stopped if mass residual <5 per cent initial value	1·37	1·74	2·22	1·15	325
6	As case 5, but Aitken's acceleration method used after every 100 double-sweeps	1	1	1	1	150

* The computer used was a CDC7600.

procedure. The application of Aitken's acceleration method was observed not only to improve the pressure correction solution during one iteration but in some cases reduce the number of sweeps required to solve for those terms during the subsequent iterations.

The problem of obtaining convergence at high rotational speeds was further investigated for the case $Re_\theta = 2{\cdot}5\times10^{5}$, $C_w = 605$. For these conditions it was found that, although the solution did appear to be converging as the computation advanced, the rate of convergence was unacceptably slow. A number of parameters were varied to try and speed up convergence. These include the under-relaxation factors, the constant α, and the number of double-sweeps allowed in the line-by-line procedure. However none of these measures produced the desired result and so it was concluded that it was impracticable to obtain full convergence. However, to try to identify the cause of these difficulties, streamline plots for the solution at various stages of the computation were produced. The stream function (ψ), which is defined so that

$$u = -\frac{1}{r}\frac{\partial\psi}{\partial z}, \qquad w = \frac{1}{r}\frac{\partial\psi}{\partial r} \tag{25}$$

was obtained by integrating the solutions for the velocities. Streamline plots were then obtained using a standard contour plotting package. A sequence of four of these plots is shown in Figure 8. These results show that the main errors in the solution are within the 'source region'. The overall flow structure is in good agreement with that expected from the numerical studies at lower rotational speeds which will be described in a separate paper. This suggests that it may be possible to obtain useful information from the numerical results, even when convergence cannot be obtained over the whole field of flow. It is interesting to note that the variation of the solution as the iterations proceed is similar to the unstable flow

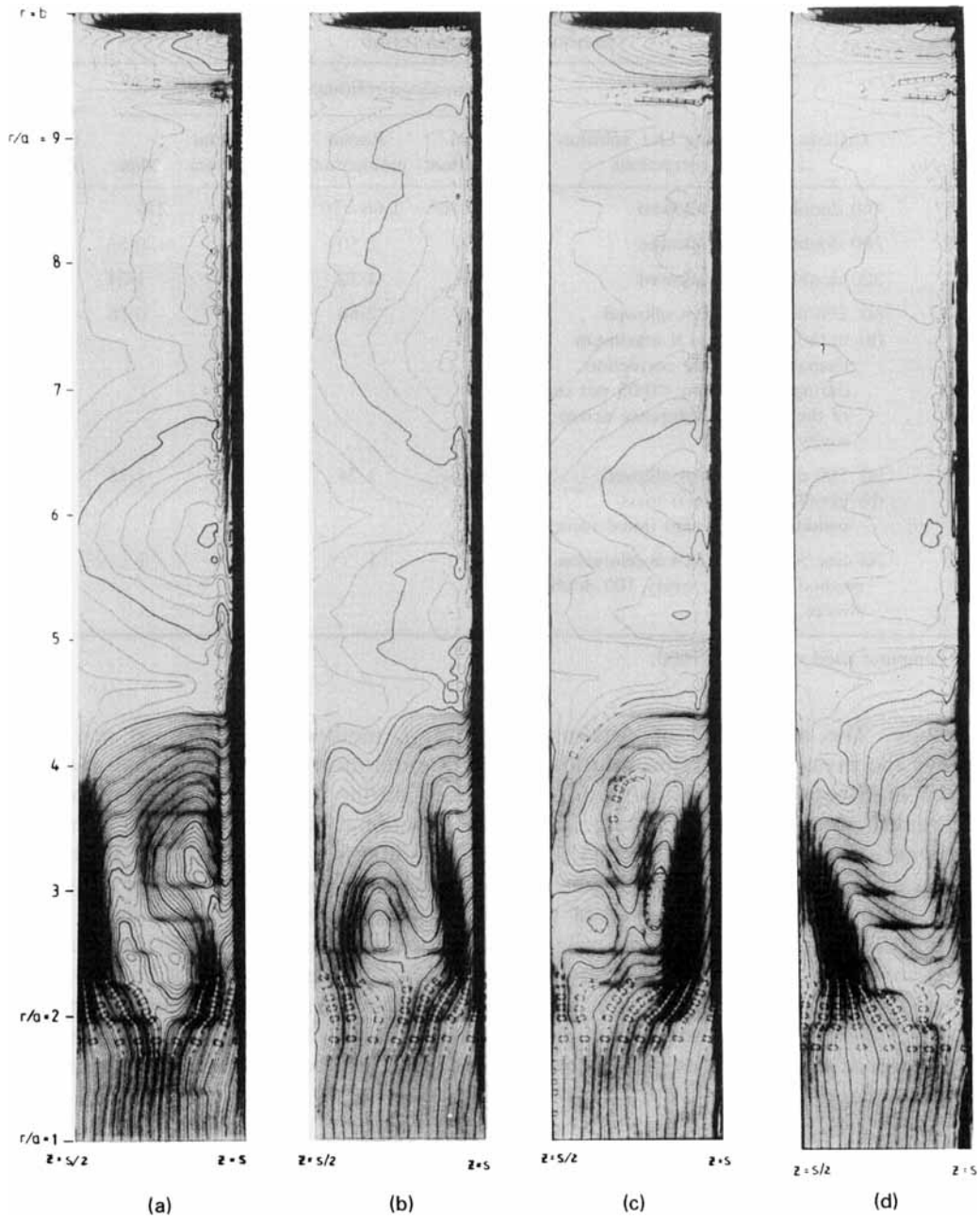

Figure 8. Radial outflow with radial inlet, $Re_\theta = 2{\cdot}5 \times 10^5$, $C_w = 605$. Streamline pattern in the half cavity $s/2 \leq z \leq s$ at different stages of the solution. Iterations completed: (a) 1100; (b) 1300; (c) 1500; (d) 1700

observed by Owen and Pincombe[1] during vortex breakdown within the source layer. Such time-dependent-like behaviour is not surprising, as a strong analogy exists between the iterative solution of the steady state equations and the transient problem (see, for example, Reference 11).

The amount of computing time used in the calculations varied considerably for different cases and was strongly dependent on the choice of the different input parameters controlling convergence. For the case $Re_\theta = 2{\cdot}5 \times 10^4$, $C_w = 0{\cdot}01$, convergence was obtained after about 20 minutes of CPU time on a CDC7600 machine. However results for other cases at the same rotational speed, but different flow rates, have been obtained in about half this time. This improvement is attributed to differences in the treatment of the pressure correction terms. For the calculations described here the program required about 70K of core store.

6. CONCLUSIONS

The numerical experiments described above illustrate some of the problems associated with the computation of rapidly rotating flows. Similar difficulties have been encountered by many other workers. The slow convergence of the numerical solution appears to be associated with instabilities in the physical flows. Just as a small physical disturbance in an experiment may propagate, so a small error in the numerical solution can lead to other errors. In the present work the Reynolds number limit for which solutions could be obtained was increased by special treatment of the pressure correction terms in the SIMPLE algorithm. The examples considered show that rotation can lead to particularly slow convergence in the solution of the pressure correction equations and, unless these equations are solved to sufficient accuracy, the errors will persist through subsequent iterations, slowing down the convergence rate or even producing divergence. It is interesting to note that Patankar[14] and Issa[15] have suggested modifications to the SIMPLE algorithm involving the pressure correction terms for non-rotating flows. Although their treatment is different from that used here there may be some link between these approaches.

The numerical results also demonstrate that a step change in mesh spacing can be successfully incorporated in the standard solution method. Using step changes in the grid to obtain sufficient resolution in the boundary layers, results have been obtained for two-dimensional source–sink flow in a rotating annulus at an order of magnitude higher Reynolds number than any previously published work for a similar type of flow.

ACKNOWLEDGEMENTS

This work was undertaken during the tenure of a Research Fellowship, supported by Rolls-Royce Limited, at the Thermo-Fluid Mechanics Research Centre, University of Sussex. I would also like to thank Dr. J. M. Owen for his comments and interest in this work.

APPENDIX: NOMENCLATURE

a	inlet radius
$\mathbf{A}$	iteration matrix in the line-by-line solution procedure
b	outer radius of cavity
$\mathbf{B}$	constant matrix in the line-by-line solution procedure
c_N, c_S, c_E, c_W	coefficients in the finite difference equations
C_w	mass flow parameter $= \dot{m}/\mu s$

$\mathbf{e}_k$	error in the pressure correction vector $= \mathbf{pp}_{\text{true}} - \mathbf{pp}_k$
$\dot{m}$	mass flow rate
p	static pressure
p'	reduced pressure $= p - \frac{1}{2}\rho\Omega^2 r^2$
pp	pressure correction
$\mathbf{pp}$	vector of pressure correction terms
Q	volumetric flow rate
r	radial distance
Re_θ	rotational Reynolds number $= b^2\Omega/\nu$
s	axial distance between the discs
S	source Reynolds number $= Q/2\pi\nu s$
S_Φ	source term in the governing equations
S_1, S_2	source terms in the finite difference equations
u, v, w	radial, tangential and axial velocity components in a cylindrical co-ordinate system (r, ϕ, z) rotating at angular speed Ω
$\mathbf{V}_i$	eigenvector of matrix $\mathbf{A}$
z	axial distance
α	constant controlling relaxation of the centrifugal force terms in the numerical solution
$\delta r, \delta z$	radial and axial grid spacings
λ_i	eigenvalue of the matrix $\mathbf{A}$
λ_s	eigenvalue of $\mathbf{A}$ with largest absolute value
μ	dynamic viscosity
ν	kinematic viscosity $= \mu/\rho$
ρ	density
ϕ	angular co-ordinate
Φ	main variable in general form of the finite difference equations
ψ	axisymmetric stream function
Ω	angular velocity of cavity

Subscripts

i, j	integers defining the position of a point on the finite difference grid
k	iteration number
N, S, E, W	pertaining to the four points immediately neighbouring P
new	value after the current iteration
old	value after the previous iteration
P	a general point on the finite difference grid
true	the exact solution

REFERENCES

1. J. M. Owen and J. R. Pincombe, 'Velocity measurements inside a rotating cylindrical cavity with a radial outflow of fluid', *J. Fluid Mech.*, **99,** 111 (1980).
2. H. P. Pao, 'A numerical computation of a confined rotating flow', *J. Applied Mechanics, TRANS ASME,* **92,** 480 (1970).
3. A. D. Gosman and D. B. Spalding, *Computation of laminar flow between shrouded rotating discs,* Department of Mechanical Engineering, Imperial College, University of London, Report No. EF/TN/A/30, 1970.
4. D. A. Bennetts and W. D. N. Jackson, 'Source–sink flows in a rotating annulus: a combined laboratory and numerical study', *J. Fluid Mech.*, **66,** 689 (1974).
5. I. Harada, 'Computation of strongly compressible rotating flows', *J. Comp. Physics,* **38,** 335 (1980).

6. P. Bar-Yoseph, J. J. Blech and A. Solan, 'Finite element solution of the Navier–Stokes equations in rotating flow', *Int. J. Num. Meth. Eng.*, **17,** 1123–1146 (1981).
7. A. D. Gosman and F. J. K. Ideriah, 'TEACH-T: a general computer program for two-dimensional turbulent recirculating flows', in *Calculation of recirculating flows*, Dept. of Mech. Eng., Imperial College, University of London, 1976.
8. A. D. Gosman, M. L. Koosinlin, F. C. Lockwood and D. B. Spalding, 'Transfer of heat in rotating systems', *ASME paper No. 76-GT-25, Gas Turbine and Fluid Eng. Conf.*, New Orleans, 1976.
9. S. V. Patankar and D. B. Spalding, 'A calculation procedure for heat, mass and momentum transfer in three-dimensional parabolic flow', *Int. J. Heat and Mass Transfer*, **15,** 1787 (1972).
10. J. W. Chew, 'Computation of flow and heat transfer in rotating cavities', *D.Phil. Thesis*, School of Engineering and Applied Sciences University of Sussex, 1982.
11. P. J. Roache, *Computational Fluid Dynamics*, Hermosa, Albuquerque, New Mexico.
12. G. D. Smith, *Numerical Solution of Partial Differential Equations: Finite Difference Methods*, 2nd Edn, Oxford University Press, 1978.
13. R. Hide, 'On source–sink flows in a rotating fluid', *J. Fluid Mech.*, **32,** 737 (1968).
14. S. V. Patankar, *Numerical Heat Transfer and Fluid Flow*, McGraw-Hill, 1980.
15. R. I. Issa, 'Numerical methods for two and three dimensional viscous flows', *Computational Fluid Dynamics*, Von Karman Institute for Fluid Dynamics, Lecture Series 1981–5, March 30–April 3.